A salmon DNA scaffold promotes osteogenesis through activation of sodium-dependent phosphate cotransporters

Yuri Katsumata, Hiroshi Kajiya*, Koji Okabe, Tadao Fukushima, and Tetsuro Ikebe

Abstract

We previously reported the promotion of bone regeneration in calvarial defects of both normal and ovariectomy-induced osteoporotic rats, with the use of biodegradable DNA/ protamine scaffold. However, the method by which this DNA-containing scaffold promotes bone formation is still not understood. We hypothesize that the salmon DNA, from which this scaffold is derived, has an osteoinductive effect on pre-osteoblasts and osteoblasts. We examined the effects of salmon DNA on osteoblastic differentiation and calcification in MC3T3-E1 cells, mouse osteoblasts, *in vitro* and bone regeneration in a calvarial defect model of aged mouse *in vivo*. The salmon DNA fragments (300 bps) upregulated the expression of the osteogenic markers, such as alkaline phosphatase, Runx2, and osterix (Osx) in MC3T3E1 cells compared with incubation with osteogenic induction medium alone. Measurement of phosphate ion concentrations in cultures showed that the DNA scaffold degraded phosphate ions were released to the cell cultures. Interestingly, we found that the inclusion of DNA in osteoblastic cell cultures upregulated the expression of sodium-dependent phosphate (NaPi) cotransporters, SLC20A1 and SLC34A2, in MC3T3-E1 cells in a time dependent manner. Furthermore, the inclusion of DNA in cell cultures increased the transcellular permeability of phosphate. Conversely, the incubation of phosphonoformic acid, an inhibitor of NaPi cotransporters, attenuated the DNA-induced expression and activation of SLC20A1 and SLC34A2 in MC3T3-E1 cells, resulting in suppression of the osteogenic markers. The implantation of a salmon DNA scaffold disk promoted bone regeneration using calvarial defect models in 30-week-old mice. Our results indicate that the phosphate released from salmon DNA upregulated the expression and activation of NaPi cotransporters, resulting in the promotion of bone regeneration.

Key words: DNA scaffold, Osteogenesis, Sodium-dependent phosphate cotransporters, Bone regeneration

1. Introduction

The engineering of efficient bone regeneration relies on three critical factors, namely, scaffolds, cells and growth factors [1, 2]. Optimal scaffolds are required to support both tissue engineered constructs and the host tissue surrounding the defect. DNA is as an interesting candidate for use in the generation of bone scaffolds, because it presents the possibility of releasing phosphates into the developing bone, which are an important constituent of the bone mineral content. The water solubility of DNA furthers the use of this material as a scaffold in bone regeneration, as it allows the gradual biodegradation of the scaffold from the implantation site within the body [3].

We recently synthesized a novel scaffold, composed of a DNA/protamine complex, by mixing an aqueous solution of salmon DNA with protamine to generate a water insoluble powder [3]. The DNA/protamine scaffold promoted new bone regeneration in rat calvarial defects via osteogenesis of the peripheral tissues surrounding the DNA/protamine scaffold [4, 5]. However, little is known about how this scaffold may promote bone regeneration.

Phosphate is the third most abundant anion in the body and required for a variety of fundamental biological processes. Inorganic phosphate is essential for bioenergetics processes (the formation of ATP and GTP), metabolic regulation in glycolysis or oxidative phosphorylation, intracellular signaling pathways (cyclic AMP and GMP), cell proliferation (DNA and RNA), and for structures such as bones and membranes [6]. Calcium phosphate forms a large component of bone minerals and as such phosphate is key to its structure. Phosphate is secreted into the bone microenvironment within matrix vesicles by osteoblasts during bone formation [7]. Furthermore, it has been reported that extracellular phosphate promotes osteogenic differentiation and calcification in pre-osteoblasts [8, 9], mesenchymal stem cells [10] and vascular smooth muscle cells [11]. Thus we hypothesize that the salmon DNA within our DNA/protamine scaffold is able to release phosphate ions to the bone microenvironment as it degrades, thereby promoting osteogenesis in pre-osteoblasts and osteoblasts.

The aim of the present study was to clarify whether the salmon DNA and its released phosphate ions contribute to osteoblastic differentiation, calcification and bone regeneration. We have investigated the effects of salmon DNA on osteoblastic differentiation and calcification in MC3T3-E1 cells, mouse osteoblasts, *in vitro* and on bone healing in calvarial defects in 30-week-old mice *in vivo*.

2. **Materials and methods**

2.1. Cell Culture

Mouse osteoblast MC3T3-E1 cells were seeded at a density of 1×10^5 cells/ml and cultured in α-minimal essential medium (α-MEM; Sigma, St. Louis, MO, USA) containing 10% fetal bovine serum (FBS) for 1, 2, 3, 5 and 7 days at 37°C and 5% CO_2. On reaching sub-confluence, cells were cultured in α-MEM with 10% FBS supplemented with bone morphogenic protein (BMP)-4 (10 ng/ml; PeproTech. Inc., NJ, USA) or osteogenic induction medium (OIM, ascorbic acid (50 μg/ml), dexamethasone (10^{-6} M) and β-glycerophosphate (10 mM)). The cells were incubated in culture medium with or without salmon DNA fragments (300 bps) for 0–7 days. In some experiments, cells were incubated in culture medium supplemented with phosphonoformic acid (PFA, 400 μM).

2.2. Alkaline phosphatase (ALP) and Alizarin red staining

After incubation for each time period with OIM in the presence or absence of salmon DNA fragments, the cells were washed twice with PBS and stained with an ALP kit (Takara Bio Inc., Ohtsu, Japan), according to the manufacturer's instructions. In parallel experiments, the cells were washed twice with PBS and fixed in 4% paraformaldehyde for 10 min. The cells were then stained with 1% alizarin red solution for 5 min.

2.3. RNA isolation and reverse-transcription polymerase chain reaction (PCR)

Total RNA was extracted from cells using the TRLzol reagent. First-strand cDNA was synthesized from 3 μg of total RNA using SuperScript II reverse transcriptase, according to the manufacturer's instructions (Invitrogen Carlsbad, CA, USA). To detect mRNA expression, we selected specific primers based on the nucleotide sequence of the resultant cDNA. Relative mRNA expression was normalized as the ratio of alkaline osteogenesis and phosphate co-transporter mRNAs to β-actin expression levels. All reactions were run in hexaplicate.

2.4. Western blot analysis

Cells were lysed in TNT buffer (Roche, Basel, Switzerland). Protein content was measured with a protein assay kit (Pierce, Hercules, CA, USA). Twenty micrograms of each protein was subjected to 12.5% sodium dodecyl sulfate polyacrylamide gel electrophoresis, and separated proteins were then electrophoretically transferred to PVDF membrane at 75 V for 1.5 h at 4°C. The membrane was incubated with the antibodies against ALP, Runx2, Osterix, SLC20A1 (Abcam, Tokyo, Japan), β-actin (Sigma Chem., St. Louis , MO, USA), SLC34A2 (Cell Signaling Technology, Inc), diluted 1:500.in 5% skimmed milk TBST (10 mM tris-HCl, 50 mM, NaCl 0.25% Tween-20) plus 0.01% azide overnight at 4°C. Blots were washed in TBST, then incubated for 1 h with horseradish peroxidase-conjugated anti-rabbit or mouse IgG secondary antibodies diluted 1:2000.in 5% skimmed milk TBST and developed using an enhanced chemiluminescence system (GE Healthcare, Tokyo, Japan).

2.5. Phosphate concentration measurements

The upper chamber of cell culture well inserts (8-μm pore size; PET track-etched membrane) were used to culture MC3T3-E1 cells in α-MEM with 10% FBS. After cells reached confluence, the upper chambers contained the cells on top of the feeder plate in α-MEM with 10% FBS and DNA fragments (300 μg/ml) and were incubated for 0, 1, 3, 5, and 7 days at 37°C. In some experiments, MC3T3- E1 cells in the upper chamber were incubated in the presence or absence of PFA (400 μM). The level of phosphates released into the culture medium on 0, 1, 3, 5, and 7 days was determined by use of Phosphor C a phosphate assay kit (Wako, Osaka, Japan) according to the manufacturer's recommended protocol.

2.6. *Preparation of DNA scaffold disks*

DNA (MW = 4500) of sterilized salmon testis was provided by Maruha-Nichiro Holdings, Ltd., Tokyo, Japan. Freeze-dried DNA powder was kneaded in distilled water to convert it into a jelly. To avoid rapid biodegradability, DNA scaffold disks were made from high molecular salmon DNA, but not DNA fragments

(300 bp). The DNA jelly was injected into a silicone mold (internal diameter: 5 mm; height: 0.8 mm) on a polytetrafluoroethylene plate. The fabricated DNA disks (40 mg) were subsequently immediately and carefully removed from the polytetrafluoroethylene plate and silicone mold.

2.7. Micro-computed tomography (μ-CT) *analysis*

Micro-CT images were taken using *in vivo* μ-CT equipment (Skyscan-1176; Bruker, Belgium) at 50 kV and 500 μA. The thickness of one μ-CT slice was 35 μm. The percentage of new bone formation in the defect area was obtained from each μ-CT image and calculated as the area of newly formed bone/area of the original defect created by trephination, in accordance with our previous paper[4]. At first, the newly formed bone area on the μ-CT slice images in the horizontal direction was quantified two-dimensionally using WINROOF image analysis software (Mitani Corp., Tokyo, Japan). The 5 mm diameter circles were drawn on each μ-CT slice image for analysis. A series of ten μ-CT images, showing areas of the highest amount of new bone formation, were used for one sample analysis. The percentage of new bone formation in the defect (% of new bone) was calculated as the total area of new bone formation per 10 μ-CT slice images ×100. All animals were treated according to the ethical regulations for animal experimentation defined by the Animal Care Committee of the Fukuoka Dental College, Fukuoka, Japan.

2.8. Statistical analysis

Data are expressed as mean ± standard error of the mean (SEM). Differences were analyzed by one-way analysis of variance (ANOVA) and Scheffe's multiple comparison tests. *P*-values of <0.05 were considered to be significant.

2.9. Reagents

Recombinant human BMP-4 was purchased from Peprotec Co. Ltd (Minneapolis, MN, USA). Anti--alkaline phosphatase, anti-Sp7/osterix, anti-HSF1, and anti-HSF2 antibodies were purchased from Abcam (Tokyo,

Japan). All other antibodies were purchased from Cell Signaling Technologies (Delaware, CA, USA). All other chemicals were obtained from Sigma Chemical Co. (St. Louis, MO, USA).

3. Results

3.1. Salmon DNA significantly promoted osteogenesis in MC3T-3E1cells.

We recently reported that the DNA/protamine disk scaffold is a new osteoinductive scaffold, which was shown to promote bone regeneration using calvarial defect model rats [4, 5]. However, little is known about how the scaffold, particularly the salmon DNA component is associated with bone regeneration. We first examined the effect of salmon DNA fragments (300 bp) on osteoblast differentiation and calcification in MC3T3-E1 cell mouse osteoblasts. Cells were incubated with OIM or treated with BMP-4 (10 ng/ml). The addition of DNA fragments (300 μg/ml) in OIM cultivation significantly increased the expression of osteogenic genes, such as ALP, Runx2, and osterix mRNAs in MC3T3-E1 cells in a time-dependent manner (Fig. 1A). Following 5 days of culture a significant upregulation of osteogenic genes was observed in the presence of >100μg/ml DNA fragments compared with OIM alone. Similarly, protein expression of osteogenic markers was upregulated on day 3 after treatment with DNA, whereas protamine alone had little effect (data not shown). Treatment with BMP-4 (10 ng/ml) also increased expression of these osteogenic related proteins in a time-dependent manner. Furthermore, incubation with DNA increased the number of cells positive for ALP activity and alizarin-stained calcium deposition in a time-dependent manner, indicating that incubation with DNA upregulated osteogenesis in osteoblast cultures (Fig. 1C).

3.2 DNA upregulated the expression and activity of sodium-dependent phosphate (NaPi) cotransporters.

In the present experiments, the DNA fragments gradually released phosphate ions during cultivation. The concentration of phosphate ions increased to 300 μg/ml on day 5 after the addition of DNA

fragments, compared with only 84 μg/ml of phosphate ions present in standard culture medium, as assessed by ion chromatographic analysis. Bone is formed by the deposition of crystals of calcium phosphate (bone minerals) among collagen fibers (bone matrix). Thus, we hypothesize that the increased concentration of phosphate ions released from the DNA in the culture medium promotes the formation of bone mineralization. It has been reported that sodium-dependent phosphate (NaPi) cotransporters are associated with phosphate uptake into osteoblasts during bone formation [7-9]. Interestingly, we found that addition of salmon DNA to MC3T3-E1 cell cultures increased the expression of NaPi cotransporters including SLC20A1 and SLC34A2 in a time-dependent manner, but expression of SLC34A1 was unchanged (Fig. 2A and 2B). Immunocytochemical analysis of SLC20A1 and SLC34A2 expression showed that DNA induction of these proteins resulted in their localization to the plasma membrane of MC3T3-E1 cells (Supplemental Fig.1). Both SLC20A1 and SLC34A2 have been associated with the deposition of bone matrix in mammalian cells [12], which is a role performed by osteoblasts [9]. In support of this we observed that pretreatment of cell cultures with phosphonoformic acid (PFA; 400 μM), an inhibitor of NaPi cotransporters, partially suppressed the DNA-induced upregulation of the SLC proteins, as well as ALP and Runx2 expression in MC3T3-E1 cells (Fig. 2C).

To clarify whether the addition of DNA to MC3T3-E1 cell cultures affects the transport of phosphate in these cells, we examined the net transcellular permeability of phosphate associated with SLCs in MC3T3-E1 cells by use of a transwell culture method (Fig. 3A). Although the phosphate concentration was almost constant in both the upper chamber and lower well during cultivation with α-MEM medium alone, the addition of DNA to the upper chamber increased the phosphate concentration in the lower well as well as the phosphate concentration released from DNA in a time-dependent manner (Fig. 3B). The addition of DNA into the upper chamber significantly increased the transcellular movement of phosphate ions between the upper chamber and lower well, via the osteoblastic layer in a time-dependent manner, compared with OIM

cultivation alone. Furthermore, the pretreatment of PFA suppressed the DNA-induced phosphate transcellular movement of phosphates in MC3T3-E1 cells, suggesting that the reduction in phosphate gradient across the transwell culture layer was partially caused by the upregulation of SLC20A1 and SLC34A2, to transport phosphate ions across the MC3T£-E1 culture layer.

3.3. DNA promotes bone regeneration using calvarial defect model mice.

To clarify whether the presence of our DNA scaffold induced bone deposition *in vivo*, we examined the effect of DNA implantation on bone regeneration in the calvarial defects model using aged ddY mice. New bone regeneration in the presence or absence of DNA scaffolds was evaluated by analysis of the calvarial defects model of 30-week-old mice. Although the calvarial defects in aged mice has been previously reported not to undergo spontaneous healing 1 month after cranial surgery [13], the defects in the present study underwent some level of regeneration (15.05±4.1 % of bone generation) 3 months after cranial surgery in the non-implanted calvarial defects in mice (empty; Fig. 4A and 4B). DNA scaffold implantation significantly induced large peninsula-like bone deposition in both horizontal and coronal directions, compared with the control (empty).

4. Discussion

Optimal scaffold designs are essential for efficient bone regeneration within the bone tissue engineered constructs and the host tissues surrounding these defects. A key feature of any scaffold must be the ability to deliver osteoinductive growth factors [14] required to stimulate the osteoblastic cells that are recruited to a bone repair site, in order to upregulate the osteogenesis activation pathway [15]. Scaffolds used in bone regeneration serve as a temporary matrix for cell migration, cell proliferation and differentiation and subsequent bone growth until a new bone tissue is totally regenerated [16]. In the present experiments, the implantation of salmon DNA disk scaffolds promoted bone regeneration compared with controls using the calvarial defects model even in 30-week-old mice. Furthermore, we have shown that the addition of DNA fragments

to osteoblast cell cultures *in vitro* upregulated osteoblastic differentiation and calcification, via activation of sodium-dependent phosphate (NaPi) cotransporters, SLC20A1 and SLC34A2.

Phosphate is essential for may vial function [17]. Our data indicated that the salmon DNA was gradually released to phosphates and increased phosphate concentration in the osteoblastic microenvironment. The transcellular uptake of phosphates has been reported to occur primarily in the proximal kidney and distal small intestine via SLCs family [18-21]. SLC34A1 and SLC34A3 are found in the proximal tubule of nephrons, while phosphate absorption in the small intestine is performed by SLC34A2. Furthermore, the broad tissue distribution of SLC20A1 and SLC20A2 has been known to serve a housekeeping role for cellular phosphate homeostasis [22]. These SLCs are associated with epithelial transcellular phosphate fluxes in kidney and intestine, and are co-expressed in several cells producing calcified tissues. Moreover, extracellular phosphate has been reported to be regulated by the expression of NaPi cotransporters, such as SLC 20A and SLC34A families [10, 22-24].

In the present experiments, we found that the addition of DNA to MC3T3-E1 osteoblast cultures upregulated the expression of two types of SLCs, SLC20A1 and SLC34A2, suggesting that these SLCs are associated with the released phosphates from salmon DNA. These SLCs were shown to be detected in membrane regions of MC3T3-E 1 cells using immunocytochemistry.

At the same time the DNA showed a two-fold increase in the transcellular phosphate permeability compared with incubation with OIM alone in MC3T3-E1 cells. Furthermore, the increase in phosphate permeability and SLC expression was attenuated by PFA, an inhibitor of NaPi cotransporters, suggesting that the transcellular permeability of phosphates is correlated with the activation of the two SLCs. Thus, the results suggest that the ability of phosphate to signal the induction of osteogenic genes and mineralization in calcified tissues is dependent upon the upregulation of the phosphate transport system.

Studies on SLCs expressed in osteoblasts have thus far been limited to the ubiquitously expressed SLC20A1 and 20A2 [25-27]. It was recently shown that BMP-2 enhanced mineralization and

phosphate uptake in MC3T3-E1 cells through an induction of SLC20A1 [28]. This stimulatory effect, but not basal mineralization, was blocked by addition of an RNAi to SLC20A1, showing that the cotransporter is also of importance for osteoblast mineralization. However, the stimulation could also be blocked by PFA at a concentration that would have no inhibitory effect on SLC20A1, suggesting that the increase in mineralization is also involved in SLC34A in MC3T3-E1. Our data suggest that SLC34A are responsible for most phosphate cotransport in mineralization, but stimulation with osteogenic factors might require the expression of SLC20A1.

In conclusion, the addition of salmon DNA to cell cultures increased the level of phosphate concentration within the microenvironment of MC3T3-E1 cells, resulting in the upregulation of SLC20A1 and SLC34A2 expression. Therefore, upregulation of SLC20A1 and 34A2 expression seems to be an essential mechanism of DNA to activate bone regeneration in osteoblasts.

Acknowledgments

This work was supported by a Grants-in-Aid for Scientific Research from the Ministry of Education, Culture, Sports, Science and Technology of Japan (No. 15K11062). We would like to thank Maruha-Nichiro Corporations for providing the DNA. The authors have declared that no conflicts of interest exist.

References

[1] B. Doll, C. Sfeir, S. Winn, J. Huard, J. Hollinger, Critical aspects of tissue-engineered therapy for bone regeneration, Crit Rev Eukaryot Gene Expr. 11 (2001) 173-198.

[2] Y. Tabata, Tissue regeneration based on growth factor release, Tissue Eng. 9 (2003) 5-15.

[3] T. Fukushima, J. Ohno, T. Hayakawa, R. Imayoshi, M. Kawaguchi, Y. Doi, K. Kanaya, M. Mitarai, Polycationic protamine for water-insoluble complex formation with DNA, Dent Mater J. 29(2010) 529-535.

[4] Y. Shinozaki, T. Yanagi, Y. Yamaguchi, H. Kido, T. Fukushima, Osteogenic evaluation of DNA/Protamine complex paste in rat cranial defects, Journal of Hard Tissue Biology 22 (2013)401-408.

[5] M. Toda, J. Ohno, Y. Shinozaki, M. Ozaki, T. Fukushima, Osteogenic potential for replacing cells in rat cranial defects implanted with a DNA/protamine complex paste, Bone 67 (2014) 237-245

[6] PC. Brazy, LJ. Mandel, SR. Gullans, SP. Soltoff, Interactions between phosphate and oxidative metabolism in proximal renal tubules, Am J Physiol. 247 (1984) 575-581.

[7] C. Montessuit, JP. Bonjour, J. Caverzasio, Expression and regulation of Na-dependent P(i) transport in matrix vesicles produced by osteoblast-like cells, J Bone Miner Res. 10(1995) 625-631.

[8] GR. Beck Jr, B. Zerler, E. Moran, Phosphate is a specific signal for induction of osteopontin gene expression, Proc Natl Acad Sci U S A. 97 (2000) 8352-8357.

[9] P. Lundquist, H. Murer, J. Biber, Type II Na+-Pi cotransporters in osteoblast mineral formation: regulation by inorganic phosphate, Cellular Physiology and Biochemistry 19(2007)43-56.

[10] YR. Shih, Y. Hwang, A. Phadke, H. Kang , NS. Hwang, EJ. Caro, S. Nguyen, M. Siu, EA. Theodorakis, NC. Gianneschi, KS. Vecchio, S. Chien, OK. Lee, S. Varghese, Calcium phosphate-bearing matrices induce osteogenic differentiation of stem cells through adenosine signaling, Proc Natl Acad Sci U S A. 111(2014) 990-995.

[11] A. Montes de Oca, JA. Madueño, JM. Martinez-Moreno, F. Guerrero, J. Muñoz-Castañeda, ME. Rodriguez-Ortiz, FJ. Mendoza, Y. Almaden, I. Lopez, M. Rodriguez, E. Aguilera-Tejero, OA. Montes de, High-phosphate-induced calcification is related to SM22α promoter methylation in vascular smooth muscle cells, J Bone Miner Res. 25 (2010) 1996-2005.

[12] IC. Forster, N. Hernando, J. Biber, H. Murer, Phosphate transporters of the SLC20 and SLC34 families, Mol Aspects Med. 34 (2013) 86-95.

[13] MD. McKee, A. Nanci, Osteopontin at mineralized tissue interfaces in bone, teeth, and osseointegrated implants: ultrastructural distribution and implications for mineralized tissue formation, turnover, and repair, Microsc Res Tech. 1 (1996) 141-164.

[14] H. Seeherman, The influence of delivery vehicles and their properties on the repair of segmental defects and fractures with osteogenic factors, J Bone Joint Surg Am. 83 (2001) 79-81.

[15] AJ. Salgado, OP. Coutinho, RL. Reis, Bone tissue engineering: state of the art and future trends, Macromolecular Bioscience 9 (2004) 743-765.

[16] DW. Hutmacher, Scaffolds in tissue engineering bone and cartilage, Biomaterials 21 (2000) 2529-2543.

[17] M. Crook, P. Tutt, P. Eldridge, R. Swaminathan, M. Crook, A case of creatine kinase non-M activity in human plasma, Ann Clin Biochem. 33 (1996) 167-170.

[18] T. Berndt, R. Kumar, Novel mechanisms in the regulation of phosphorus homeostasis, Physiology (Bethesda) 24 (2009) 17-25.

[19] H. Murer, I. Forster, J. Biber, The sodium phosphate cotransporter family SLC34, Pflügers Archiv 447 (2004) 763-767.

[20] H. Murer, N. Hernando, I. Forster, J. Biber, Proximal tubular phosphate reabsorption: molecular mechanisms, Physiol Rev. 80 (2000) 1373-1409.

[21] A. Werner, L. Dehmelt, P. Nalbant, Na^+-dependent phosphate cotransporters: the NaPi protein families, The Journal of Experimental Biology 201 (1998) 3135-3142.

[22] MP. Kavanaugh, DG. Miller, W. Zhang, W. Law, SL. Kozak, D. Kabat, AD. Miller, Cell-surface receptors for gibbon ape leukemia virus and amphotropic murine retrovirus are inducible sodium-dependent phosphate symporters, Proc Natl Acad Sci U S A. 19 (1994) 7071-7075.

[23] CM. Giachelli, Vascular calcification mechanisms, J Am Soc Nephrol. 15(2004) 2959-2964.

[24] ML. Chien, JL. Foster, JL. Douglas, JV. Garcia, The amphotropic murine leukemia virus receptor gene encodes a 71-kilodalton protein that is induced by phosphate depletion, Journal of Virology 71(1997) 4564-4570.

[25] LB. Nielsen, FS. Pedersen, L. Pedersen, Expression of type III sodium-dependent phosphate transporters/retroviral receptors mRNAs during osteoblast differentiation, Bone 28(2001) 160-166.

[26] G. Palmer, JP. Bonjour, J. Caverzasio, Expression of a newly identified phosphate transporter/retrovirus receptor in human SaOS-2 osteoblast-like cells and its regulation by insulin-like growth factor I, Endocrinology 138 (1997) 5202-5209.

[27] E. Zoidis, C. Ghirlanda-Keller, M. Gosteli-Peter, J. Zapf, C. Schmid, Regulation of phosphate (Pi) transport and NaPi-III transporter (Pit-1) mRNA in rat osteoblasts, Journal of Endocrinology 181 (2004) 531-540.

[28] A. Suzuki, C. Ghayor, J. Guicheux, D. Magne, S. Quillard, A. Kakita, Y. Ono, Y. Miura, Y. Oiso, M. Itoh, J. Caverzasio, Enhanced expression of the inorganic phosphate transporter Pit-1 is involved in BMP-2-induced matrix mineralization in osteoblast-like cells, Journal of Bone and Mineral Research 21 (2006) 674-683.

Figure legends

Fig. 1. The addition of salmon DNA fragments (300 bps, 300 μg/ml) significantly promoted osteogenesis in MC3T3-E1 cells compared with controls.

(A) Expression of osteogenic genes, ALP, Runx2 and OSX (osterix) in MC3T3-E1 cells following DNA treatment. Samples were analyzed by quantitative RT-PCR and normalized to β-actin mRNA. Data shown are the mean from six culture wells (mean±SEM). * and ** indicate $p<0.05$ and $p < 0.01$, versus control (incubation with only OIM). (B) Western blotting carried out using targeted and β-actin antibodies in MC3T3-E1. Similar results were obtained in five independent experiments. (C) The cells were treated with BMP-4 (10 ng/ml) in the presence and absence of DNA and stained with ALP and Alizarin red for the indicated times. The panels indicate ALP and Alizarin red staining images for the indicated times with or without DNA incubation, respectively. Similar results were obtained in five independent experiments.

Fig. 2. Incubation with DNA upregulated the expression and activation of sodium-dependent phosphate (NaPi) cotransporters, including SLC20A1 and SLC34A2 in MC3T3-E1 cells.

(A) Expression of NaPi cotransporters, SLC20A and SLC34A were analyzed by quantitative RT-PCR in MC3T3-E1 cells following incubation with DNA, Results were normalized to β-actin mRNA. Data shown are the mean from six culture wells (mean±SEM). ** indicate $p < 0.01$, versus OIM group. (B) Western blotting carried out using antibodies targeted to the SLC family and β-actin in MC3T3-E1. Similar results were obtained in five independent experiments. (C) The effects of phosphonoformic acid (PFA; 400 μM), an inhibitor of NaPi cotransporters, on the expression of osteogenesis and SLC expression. MC3T3-E1 cells were incubated with DNA before and 6h after treatment with PFA. Similar results were obtained in five independent experiments.

Fig. 3. Incubation of MC3T3-E1 cells with DNA fragments increased the transcellular permeability to phosphates and was attenuated by phosphonoformic acid.

(A) MC3T3-E1 cells were cultured to confluence in the upper transwell and incubated with DNA for up to 7 days. (B) MC3T3-E1 cells were incubated in control and osteoinductive media in the presence or absence of DNA and PFA (400 μM) for 0–7 days culture periods. The phosphate concentration was measured in collected medium of lower wells. Data are the mean from six culture wells (mean ± SEM). * and ** indicate $p<0.05$ and $p < 0.01$, versus control (OIM).

Fig. 4. DNA scaffold disk promoted bone regeneration in time-dependent manner using calvarial defect model mice.

(A) Coronal μ-CT images of DNA scaffold implantation at 1, 2 and 3 months after cranial surgery. The upper images represent empty implantations and the lower images represent DNA implantation samples. The white dashed circles indicate calvarial defects just after cranial surgery (5 mm in diameter). **(B)** Calculated new bone deposition rate at 1, 2 and 3 months after cranial surgery. The percentage of new bone mineral deposition was calculated from the bony tissue in the white dashed line in three-mice. Data shown are the mean from three mice (mean ± SEM). $^{**}P < 0.01$, empty vs.DNA implantation group.

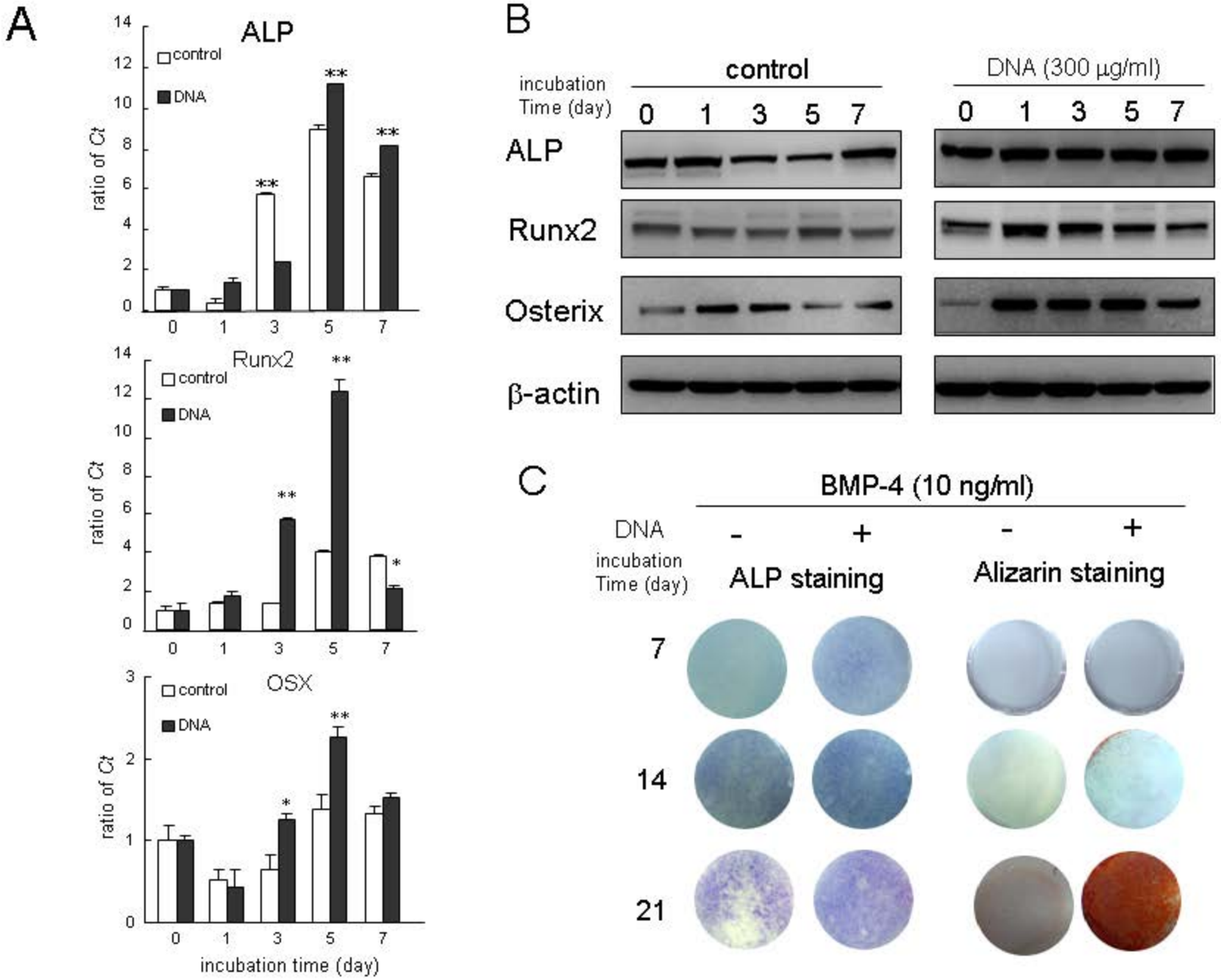
A
ALP
control
DNA
ratio of Ct
Runx2
OSX
incubation time (day)
B
control
DNA (300 μg/ml)
incubation Time (day)
0 1 3 5 7
ALP
Runx2
Osterix
β-actin
C
BMP-4 (10 ng/ml)
DNA
incubation Time (day)
ALP staining
Alizarin staining
7
14
21

Fig. 1

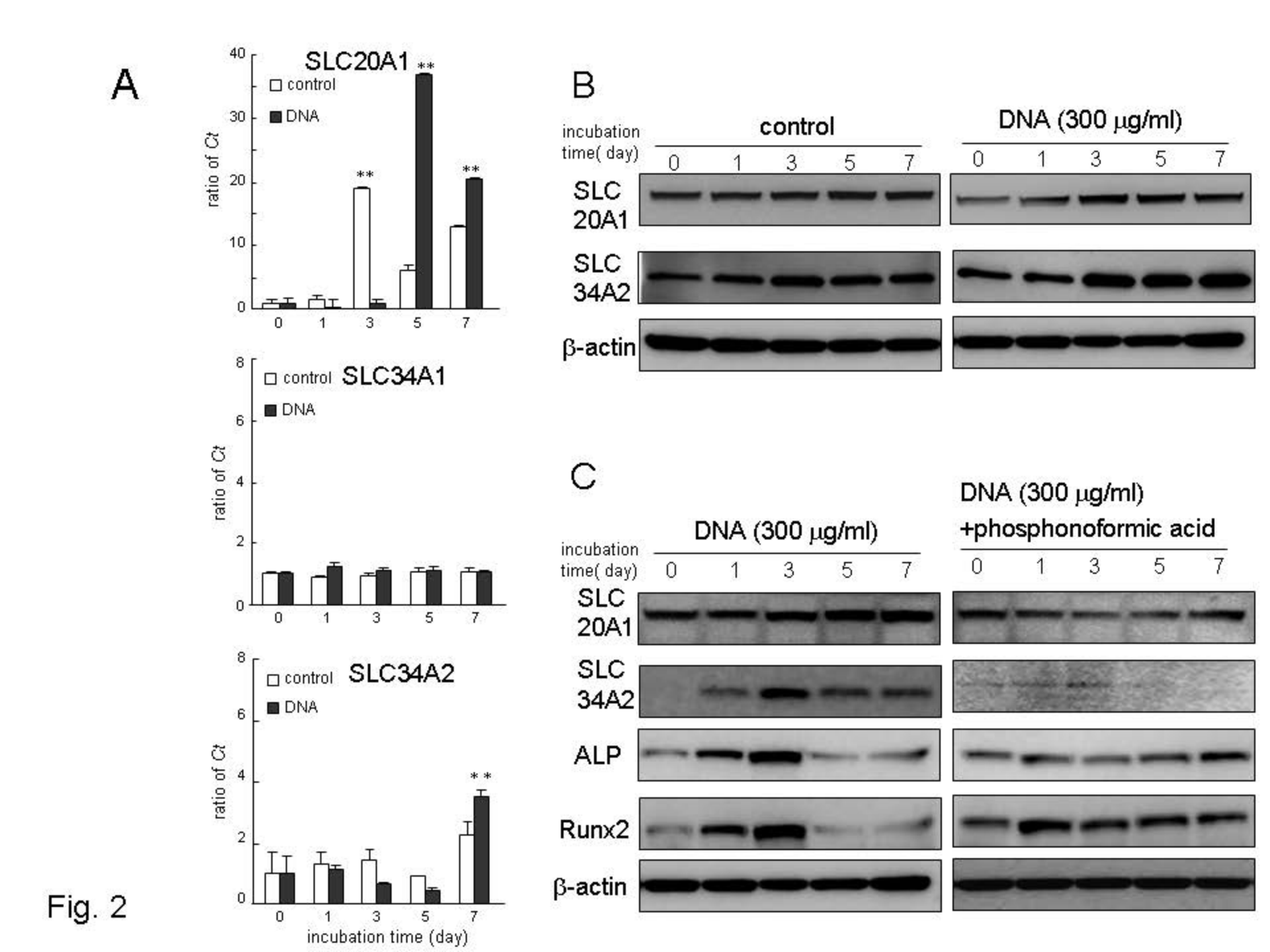
A
SLC20A1
control
DNA
ratio of Ct
40
30
20
10
0
0 1 3 5 7
**
**
**
SLC34A1
control
DNA
ratio of Ct
8
6
4
2
0
0 1 3 5 7
SLC34A2
control
DNA
ratio of Ct
8
6
4
2
0
0 1 3 5 7
* *
incubation time (day)
B
incubation time(day)
control
DNA (300 μg/ml)
0 1 3 5 7
0 1 3 5 7
SLC 20A1
SLC 34A2
β-actin
C
DNA (300 μg/ml)
DNA (300 μg/ml) +phosphonoformic acid
incubation time(day)
0 1 3 5 7
0 1 3 5 7
SLC 20A1
SLC 34A2
ALP
Runx2
β-actin

Fig. 2

A

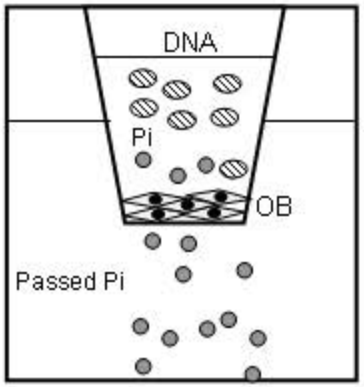
DNA
Pi
OB
Passed Pi

B

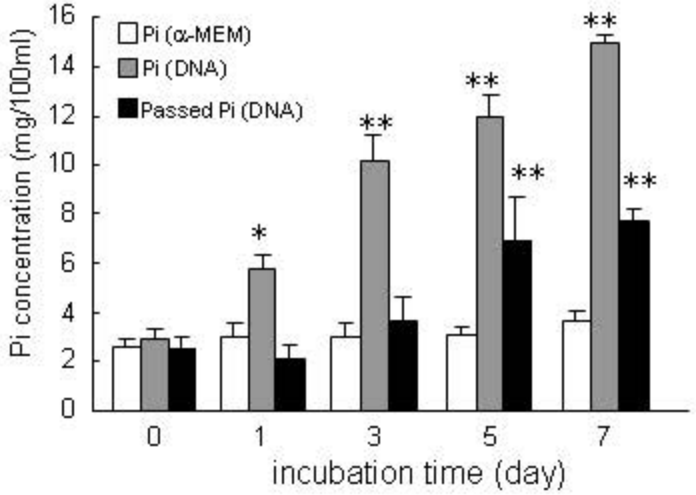
Pi (α-MEM)
Pi (DNA)
Passed Pi (DNA)
Pi concentration (mg/100ml)
incubation time (day)

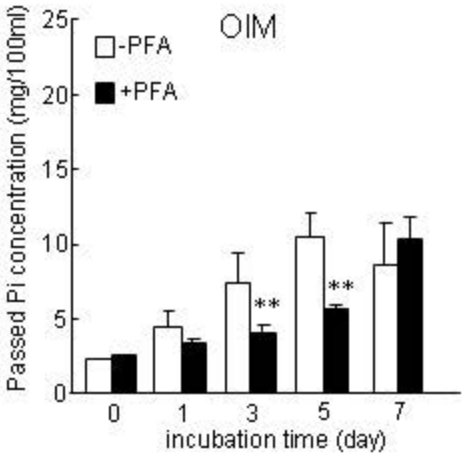
OIM
-PFA
+PFA
Passed Pi concentration (mg/100ml)
incubation time (day)

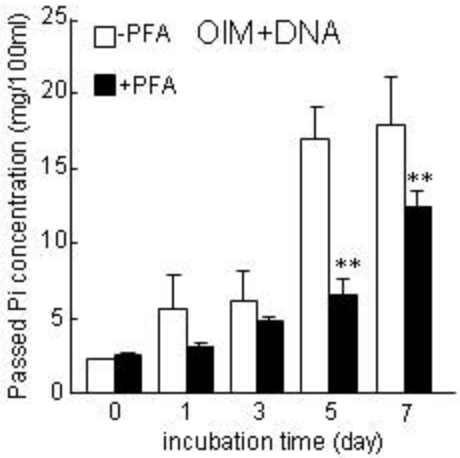
OIM+DNA
-PFA
+PFA
Passed Pi concentration (mg/100ml)
incubation time (day)

Fig. 3

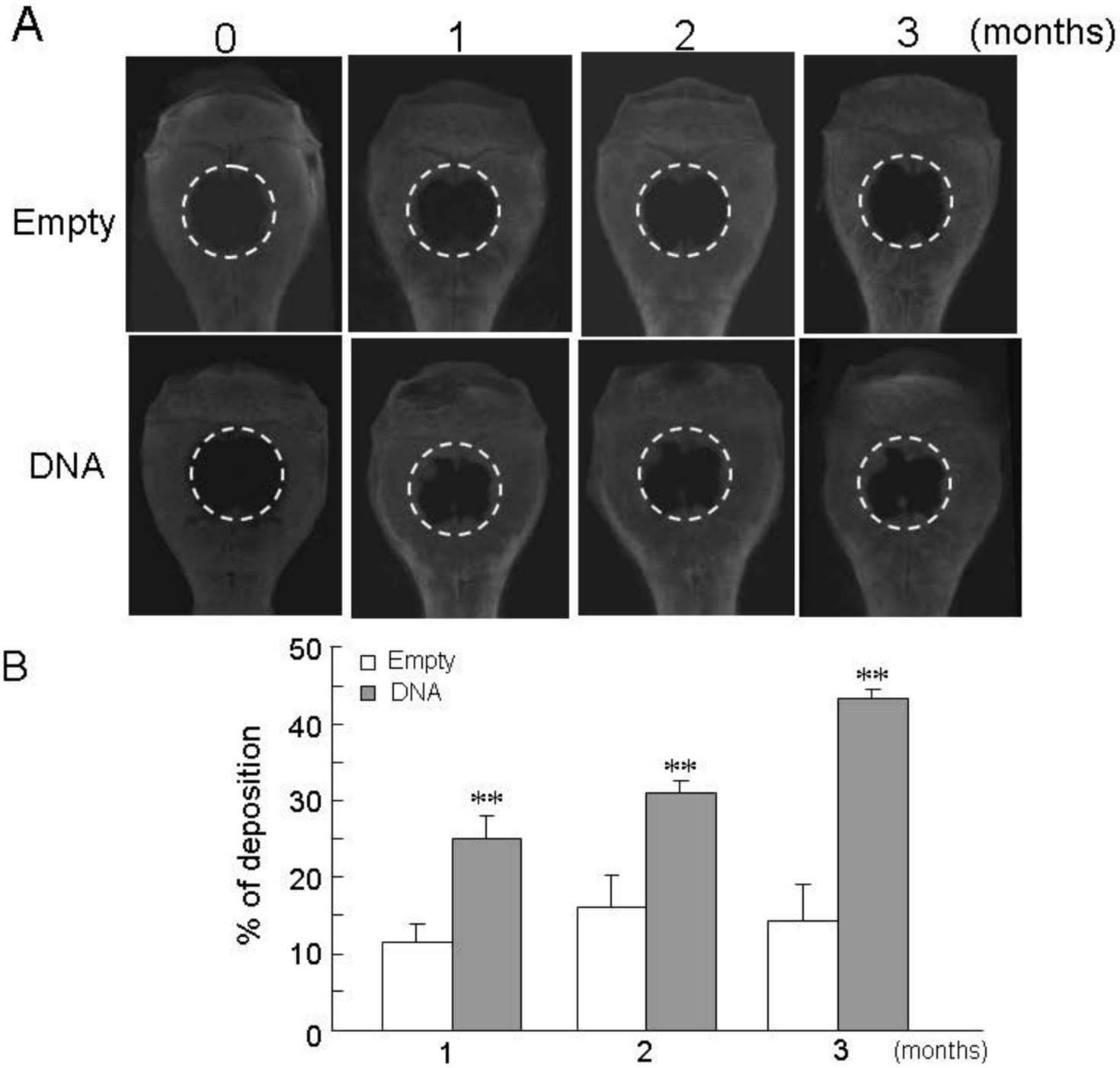
A
0
1
2
3
(months)
Empty
DNA
B
50
40
30
20
10
0
% of deposition
Empty
DNA
**
**
**
1
2
3
(months)

Fig. 4

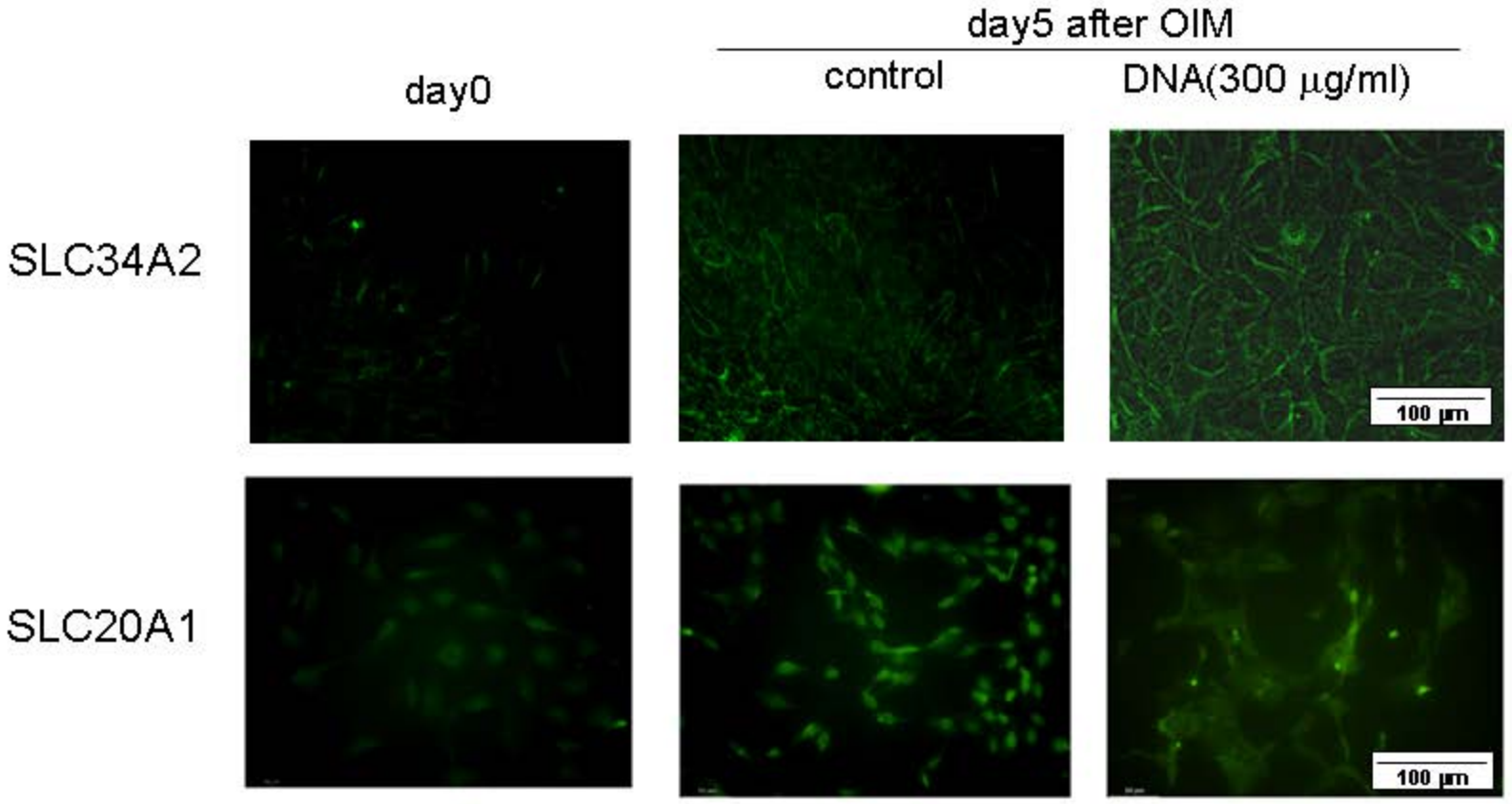

Supplemental Fig1